

TRANSMISSION AND LINE BROADENING IN THE MÖSSBAUER EFFECT. II<sup>†\*</sup>S. MARGULIES<sup>††</sup>, P. DEBRUNNER and H. FRAUENFELDER*University of Illinois, Urbana, Illinois*

Received 1 August 1962

Calculations expressing the shape of the Mössbauer line to be expected in a transmission-type experiment are extended to the case where both emission and absorption spectra are split by a hyperfine interaction. To see the effects of spectral shape, Gaussian as well as Lorentzian spectra are considered. The results indicate that the characteristics of the transmitted line are strongly dependent upon the spectral shape.

To test the calculations, the transmitted line shape was measured as a function of absorber thickness. These experiments were performed with the 14.4 keV radiation emitted by Fe<sup>57</sup>. To obtain unsplit spectra, Type 310 stainless steel was used for both source backing and absorbers. The observed line was more than four times as wide as the natural width, and was neither Lorentzian nor Gaussian. An unambiguous comparison with the calculations is therefore impossible. Averaging the results of analyses based on Lorentzian and Gaussian shapes yields  $f = 67\%$ ,  $f'_A = 137\%$  for the source and absorber recoilless fractions. Identically split spectra were obtained by using Armco iron for the source backing and the absorbers. In this case, the central resonance line was approximately Lorentzian. Applying the corresponding analysis yields  $f = 67\%$ ,  $f'_A = 144\%$ . These anomalously high values of  $f'_A$  were obtained by using a conversion coefficient of 15. To obtain reasonable values, a conversion coefficient of about 8 is required.

## 1. Introduction

In less than four years the Mössbauer effect<sup>1,2)</sup> has become a major tool in modern physics. A large number of papers have appeared in areas as diverse as relativity and chemistry<sup>3,4)</sup>. Because of this great concentration of effort, techniques and procedures have rapidly improved to the point where almost the full sensitivity inherent in the Mössbauer effect is available. The very narrow resonance lines ( $10^{-10}$  to  $10^{-5}$  eV) resulting from gamma-ray transitions from metastable nuclear levels are measured, and line widths approaching the natural widths of the transitions have been observed. As a consequence of the refined methods now available, a consideration of the details of the line shape to be expected is of interest. For example, a study of broadened lines may shed light upon the solid-state phenomena that cause the broadening.

The shape of the Mössbauer line to be expected in a transmission-type experiment<sup>2)</sup> is discussed in a previous paper<sup>5)</sup>. There, an integral expressing the transmission of resonance radiation emitted from a source of finite thickness and passing through an external resonance absorber is examined. In the present work, these calculations are extended to the case where the emission and absorption lines are split by a hyperfine interaction. In addition, to see the effects of spectral shape, Gaussian as well as the usual Lorentzian spectra are considered. Finally, the results of a series of line-shape measurements using the Fe<sup>57</sup> 14.4 keV radiation are presented and interpreted with the aid of the calculations.

<sup>†</sup> This work has been supported by the Office of Naval Research.

<sup>\*</sup> Based on a thesis (S. Margulies) submitted in partial fulfillment of the requirements for the degree of Doctor of Philosophy.

<sup>††</sup> Present address: Max-Planck-Institut für Kernphysik, Heidelberg, Germany.

<sup>1)</sup> R. L. Mössbauer, *Z. Physik* **151** (1958) 124. Reprinted in ref.<sup>3)</sup>.

<sup>2)</sup> R. L. Mössbauer, *Naturwissenschaften* **45** (1958) 538. Reprinted in ref.<sup>3)</sup>.

<sup>3)</sup> H. Frauenfelder, *The Mössbauer Effect* (W. A. Benjamin, Inc., New York, 1962).

<sup>4)</sup> A. Schoen and D. M. J. Compton, Eds., *Proc. Second Mössbauer Conf., Paris, 1961* (John Wiley, New York, 1962).

<sup>5)</sup> S. Margulies and J. R. Ehrman, *Nucl. Instr. and Meth.* **12** (1961) 131. Reprinted in ref.<sup>3)</sup>.

## 2. Theory

### 2.1. GENERAL FORMULATION

Although experiments involving the Mössbauer effect can be performed with either a transmission or a scattering geometry, most of the work done so far has employed the former approach. A typical transmission experiment consists of measuring the resonance radiation passing through a resonance absorber as a function of the relative velocity between source and absorber. To calculate the transmitted intensity, the geometry and the notation established in ref.<sup>6)</sup> will be employed. Thus,  $f$  represents the fraction of gamma rays emitted without recoil energy loss. The emission and absorption spectrum of the resonance radiation is at first assumed to have Lorentzian shape. The remaining fraction  $(1-f)$  of the radiation is non-resonant, and is subject only to ordinary electronic absorption. The source is considered to have arbitrary area and to extend in depth from  $x = 0$  to  $x = \infty$ . The distribution of emitting atoms along the  $x$ -axis is denoted by  $\rho(x)$ . Only radiation emitted normal to the area of the source is discussed.

In general, both emission and absorption spectra are split because of the hyperfine interaction between the nuclear moments and the surrounding electric and magnetic fields. Consequently, an emission spectrum split into  $N_s$  components is assumed, the  $i^{\text{th}}$  component having energy  $E_i^{(s)}$  and relative intensity  $W_i^{(s)}$ . The corresponding quantities for the absorber are denoted by  $N_A$ ,  $E_j^{(A)}$  and  $W_j^{(A)}$ . It is assumed that the absorbing atoms in a source of finite thickness have the same hyperfine structure as the emitting atoms.

If the internal conversion coefficient  $\alpha$  is sufficiently large to make the re-radiated contribution negligible, then the intensity behind a resonance absorber of thickness  $t_A$  moving with velocity  $v$  and therefore having a Doppler shift  $\mathcal{S} = (v/c) E_0$  relative to the source is given by

$$\begin{aligned}
 p(\mathcal{S}) = & \frac{e^{-\mu_A t_A}}{1 + \alpha} \left\{ (1 - f) \sum_{i=1}^{N_s} W_i^{(s)} \int_0^\infty dx \rho(x) e^{-\mu_s x} + \right. \\
 & + \int_{-\infty}^\infty dE \exp \left[ - \sum_{j=1}^{N_A} W_j^{(A)} f'_A n_A a_A \sigma_0 t_A \frac{\frac{1}{4} \Gamma_A^2}{(E - E_j^{(A)} - \mathcal{S})^2 + \frac{1}{4} \Gamma_A^2} \right] \sum_{i=1}^{N_s} \frac{W_i^{(s)} / \Gamma_s}{2\pi} \int_0^\infty \frac{dx \rho(x)}{(E - E_i^{(s)})^2 + \frac{1}{4} \Gamma_s^2} \\
 & \left. \times \exp \left[ - \left( \sum_{i=1}^{N_s} W_i^{(s)} f'_s n_s a_s \sigma_0 \frac{\frac{1}{4} \Gamma_s^2}{(E - E_i^{(s)})^2 + \frac{1}{4} \Gamma_s^2} + \mu_s \right) x \right] \right\}. \quad (1)
 \end{aligned}$$

In this equation  $\sigma_0$  is the cross section at resonance<sup>6)</sup> and the subscripts S and A identify the following source and absorber quantities:

$f'$  = probability of resonance absorption without recoil,

$n$  = number of atoms per cubic centimeter of volume,

$a$  = fractional abundance of the atoms which can absorb resonantly,

$\Gamma$  = full width at half-height of the spectral lines. (In general, both  $\Gamma_s$  and  $\Gamma_A$  may differ from the natural width.)

$\mu$  = ordinary electronic absorption coefficient, evaluated at the unsplit transition energy  $E_0$ .

The first term in eq. (1) represents the transmission of the non-resonant fraction of the radiation and is independent of  $\mathcal{S}$ . In the second term, which is the resonant contribution, the  $x$  integral represents the emission and self-absorption in the source. The remaining factors represent the absorption in the external

<sup>6)</sup> The absorption cross section at resonance is given by

$$\sigma_0 = 2\pi\lambda^2 \left( \frac{2I^* + 1}{2I + 1} \right) \frac{1}{(1 + \alpha)} \frac{\Gamma}{\Gamma_A}$$

where  $2\pi\lambda$  is the wavelength of the gamma ray,  $I$  and  $I^*$  are the nuclear spins of the ground and excited states, respectively,  $\alpha$  is the conversion coefficient for the transition,  $\Gamma$  is the natural and  $\Gamma_A$  the total line width.

resonance absorber. The lower limit on the energy integral has been taken as  $-\infty$  instead of zero for convenience. Because only relative motion between source and absorber is pertinent, the Doppler shift  $-\mathcal{S}$  can be removed from the external absorber term and included in the source term as  $+\mathcal{S}$  if desired.

Since  $e^{-\mu_A t_A}$  is the non-resonant electronic absorption in the external absorber and

$$\frac{1}{(1 + \alpha)} \int_0^\infty dx \rho(x)$$

represents the effective intensity (the number of radioactive atoms which decay by gamma emission), it is convenient to deal with a normalized transmission  $P(\mathcal{S})$  defined by

$$P(\mathcal{S}) = \frac{\dot{p}(\mathcal{S})}{\frac{e^{-\mu_A t_A}}{(1 + \alpha)} \int_0^\infty dx \rho(x)}. \quad (2)$$

The transmission integral in the general form given above can not be evaluated unless the source distribution and the component spacings and amplitudes are specified. In what follows, several cases of interest are considered. To facilitate computation, source and absorber line widths will be assumed to be equal:  $\Gamma_s = \Gamma_A \equiv \Gamma'$ . The common width  $\Gamma'$  need not be equal to the natural width  $\Gamma$  provided that the factor  $\Gamma/\Gamma_A = \Gamma/\Gamma'$  is present in the expression for the cross section<sup>6)</sup>.

## 2.2. UNSPLIT SPECTRA

The special case of eq. (1) corresponding to unsplit emission and absorption spectra ( $W_1^{(s)} = W_1^{(A)} = 1$ ;  $W_i^{(s)} = W_i^{(A)} = 0$ ,  $i \neq 1$ ) is discussed in detail in ref.<sup>5)</sup>). There, the  $x$  and  $E$  integrals are numerically evaluated for both uniform ( $\rho(x) = N$  atoms/cm,  $t_s \geq x \geq 0$ ) and Gaussian ( $\rho(x) = (2N/\sqrt{\pi}) \exp[-(x/t_s)^2]$  atoms/cm,  $x \geq 0$ ) source distributions. Defining the source and absorber effective thickness as  $T_s = f'_s n_s a_s \sigma_0 t_s$  and  $T_A = f'_A n_A a_A \sigma_0 t_A$ , it is found that for  $T_s$  and  $T_A$  between zero and at least ten the transmitted line is, to a very good degree of approximation, a Lorentz curve whose full width at half-height  $\Gamma_a$  depends upon the values of  $T_s$  and  $T_A$ :

$$P(\mathcal{S}) \simeq P(\infty) - \frac{P(\infty) - P(0)}{1 + (2\mathcal{S}/\Gamma_a)^2}. \quad (3)$$

The relative line broadening  $\Gamma_a/\Gamma'$  is presented graphically for both types of source distribution for the range  $10 \geq (T_s, T_A) \geq 0$ . In the present work, the broadening will be expressed as

$$\Gamma_a = \Gamma_a(T_s, T_A) = 2\Gamma' h(T_s, T_A), \quad (4)$$

where  $h(T_s, T_A)$  differs from  $\Gamma_a/\Gamma'$  only by a factor of  $\frac{1}{2}$ .

Non-resonantly absorbing sources ( $a_s = 0$ ) are also considered in ref.<sup>5)</sup>. For such sources the transmission is given by

$$P(\mathcal{S}) = [(1 - f) + fI(\mathcal{S}; T_A)] P_{\text{non-res}}, \quad (5)$$

where

$$I(\mathcal{S}; T_A) = \frac{\Gamma'}{2\pi} \int_{-\infty}^{\infty} \frac{dE}{E^2 + \frac{1}{4}\Gamma'^2} \exp\left(\frac{-T_A \frac{1}{4}\Gamma'^2}{(E - \mathcal{S})^2 + \frac{1}{4}\Gamma'^2}\right) \quad (6)$$

<sup>6)</sup> In the analysis of ref.<sup>5)</sup>, it is assumed that emission and absorption spectra are centered about the same energy:  $E_1^{(s)} = E_1^{(A)} = E_0$ . In general, an isomeric shift may displace these spectra. Thus,  $\mathcal{S} = 0$  must be interpreted as the shift required to produce exact overlap. By  $\mathcal{S} = \infty$  is meant, of course, a shift sufficiently large so that no overlap remains.

and

$$P_{\text{non-res}} = \int_0^\infty dx \rho(x) \exp(-\mu_s x) / \int_0^\infty dx \rho(x).$$

In addition, the quantity

$$\varepsilon(0) = \frac{P(\infty) - P(0)}{P(\infty)} = f [1 - e^{-\frac{1}{2} T_A J_0(\frac{1}{2} i T_A)}] \quad (7)$$

together with the definition of  $T_A$  can be used to extract the recoilless fractions  $f$  and  $f'_A$  from experimental data<sup>8)</sup>. Because of the slow variation of  $J_0(i T_A/2)$  with  $T_A$ , the results of this method are not very precise. A more precise procedure, based upon eqs. (3), (4) and (7), and expressed in terms of the area under an absorption curve, is described by Shirley *et al.*<sup>9)</sup>.

### 2.3. EFFECTS OF HYPERFINE SPLITTING

As mentioned previously, the transmission integral of eq. (1) cannot be evaluated in its most general form. In this paper several special cases where either source, absorber, or both, have split transition lines are investigated. To simplify the problem, only non-resonantly absorbing sources are considered. Such sources can be produced, for example, by co-plating the activity together with a non-resonantly absorbing host material<sup>10)</sup>. In such cases  $a_s$  vanishes and eq. (1) reduces to

$$P(\mathcal{S}) = \left\{ (1 - f) + \sum_{i=1}^{N_s} f W_i^{(s)} \frac{\Gamma'}{2\pi} \int_{-\infty}^{\infty} \frac{dE}{(E - E_i^{(s)})^2 + \frac{1}{4} \Gamma'^2} \exp \left( - \sum_{j=1}^{N_A} \frac{\frac{1}{4} W_j^{(A)} T_A \Gamma'^2}{(E - E_j^{(A)} - \mathcal{S})^2 + \frac{1}{4} \Gamma'^2} \right) \right\} P_{\text{non-res}}. \quad (8)$$

#### 2.3.1. Split emission spectrum and unsplit absorption spectrum

When the emission spectrum is split while the absorption spectrum is not, eq. (8) becomes

$$P(\mathcal{S}) = \left\{ (1 - f) + \sum_{i=1}^{N_s} f W_i^{(s)} \frac{\Gamma'}{2\pi} \int_{-\infty}^{\infty} \frac{dE}{(E - E_i^{(s)})^2 + \frac{1}{4} \Gamma'^2} \exp \left( \frac{-\frac{1}{4} T_A \Gamma'^2}{(E - E^{(A)} - \mathcal{S})^2 + \frac{1}{4} \Gamma'^2} \right) \right\} P_{\text{non-res}}. \quad (9)$$

Here,  $W_i^{(s)}$  represents the relative intensity of the  $i^{\text{th}}$  emission line centered about the energy  $E_i^{(s)}$ ;  $E^{(A)}$  is the center energy of the single absorption line.

Often the spacing between adjacent lines is considerably greater than the line width—i.e.,  $\Gamma' \ll |E_i^{(s)} - E_{i+1}^{(s)}| \ll 1^{11)}$ . Under such circumstances appreciable absorption occurs only when the Doppler shift  $\mathcal{S}$  is such as to bring the absorption line in near coincidence with one of the emission lines, the energy integral being essentially unity otherwise.

If the total Doppler shift is written as  $\mathcal{S} = \mathcal{S}_i + \mathcal{S}'_i$ , where  $\mathcal{S}_i = E_i^{(s)} - E^{(A)}$  is the shift required for exact overlap with the  $i^{\text{th}}$  emission line and  $\mathcal{S}'_i$  is the shift relative to this value, then, in the vicinity of the  $i^{\text{th}}$  line,

$$P(\mathcal{S} = \mathcal{S}_i + \mathcal{S}'_i) = \{ (1 - f) + f \sum_{k \neq i} W_k^{(s)} + f W_i^{(s)} I(\mathcal{S}'_i; T_A) \} P_{\text{non-res}}, \quad (10)$$

for  $|\mathcal{S}'_i| \ll |E_i^{(s)} - E_{i+1}^{(s)}|$ . Here, the first term represents the transmission of the non-resonant fraction of the radiation, the second the transmission of the  $N_s - 1$  source lines which are far from resonance, while the third represents the transmission of the  $i^{\text{th}}$  emission line which is resonantly absorbed in the external absorber. The function  $I(\mathcal{S}; T_A)$  is defined in eq. (6).

<sup>8)</sup> P. P. Craig, J. G. Dash, A. D. McGuire, D. E. Nagle and R. R. Reiswig, Phys. Rev. Letters **3** (1959) 221.

<sup>9)</sup> D. A. Shirley, M. Kaplan and P. Axel, Phys. Rev. **123** (1961) 816.

<sup>10)</sup> S. S. Hanna, J. Heberle, C. Littlejohn, G. J. Perlow, R. S. Preston and D. H. Vincent, Phys. Rev. Letters **4** (1960) 28.

<sup>11)</sup> This condition is not necessary for the evaluation of eq. (9) but happens to be satisfied for the experiments performed.

Thus, each time the Doppler shift results in appreciable overlap between the single absorption line and an emission line, the transmission decreases and a resonance line appears. The shape of the line, determined by  $I(\mathcal{S}; T_A)$  is then approximately Lorentzian for  $T_A$  at least up to 10. The variation of the full width at half-height of the resulting line can be found from the  $T_s = 0$  curve of either fig. 3 or fig. 4 of ref.<sup>5</sup>).

Using the fact that  $I(\infty; T_A) = 1$ , one obtains

$$\varepsilon(\mathcal{S}_i) = \frac{P(\infty) - P(\mathcal{S}_i)}{P(\infty)} = fW_i^{(s)} [1 - e^{-\frac{1}{2}T_A} J_0(\frac{1}{2}i T_A)] . \quad (11)$$

Thus, analyses for determining the recoilless fractions but based on unsplit spectra can be used when the absorption spectrum is split while the emission spectrum is not, by employing eq. (11) in place of eq. (7). It should be noted that  $fW_i^{(s)}$  can be interpreted as the effective recoilless fraction corresponding to the  $i^{\text{th}}$  emission line.

### 2.3.2. Unsplit emission spectrum and split absorption spectrum

When the absorption spectrum is split while the emission spectrum is not, the normalized transmission becomes

$$P(\mathcal{S}) = \left\{ (1 - f) + f \frac{\Gamma'}{2\pi} \int_{-\infty}^{\infty} \frac{dE}{(E - E^{(s)})^2 + \frac{1}{4}\Gamma'^2} \exp \left( - \sum_{j=1}^{N_A} \frac{\frac{1}{4} W_j^{(A)} T_A \Gamma'^2}{(E - E_j^{(A)} - \mathcal{S})^2 + \frac{1}{4}\Gamma'^2} \right) \right\} P_{\text{non-res}} . \quad (12)$$

In this equation  $W_j^{(A)}$  is the relative intensity of the  $j^{\text{th}}$  absorption line centered about the energy  $E_j^{(A)}$  and  $E^{(s)}$  is the center energy of the single emission line.

Again, if one assumes that the absorption lines are widely separated as compared with the line width<sup>11</sup>), then resonance absorption occurs only at Doppler shifts which bring one of the absorption lines into coincidence with the source line. Writing  $\mathcal{S}$  as the sum of two terms, one obtains near the  $j^{\text{th}}$  absorption line

$$P(\mathcal{S} = \mathcal{S}_j + \mathcal{S}'_j) = [(1 - f) + fI(\mathcal{S}'_j; W_j^{(A)} T_A)] P_{\text{non-res}} , \quad (13)$$

for  $|\mathcal{S}'_j| \ll |E_j^{(A)} - E_{j+1}^{(A)}|$ . Here  $\mathcal{S}'_j = E^{(s)} - E_j^{(A)}$  is the Doppler shift required for exact overlap and  $\mathcal{S}_j$  is the shift relative to this value.

The shape of each of the transmitted lines is again determined by the function  $I(\mathcal{S}; T)$  of eq. (6). In this case, however, the effective thickness of the resonance absorber corresponding to the  $j^{\text{th}}$  absorption line is not  $T_A$ , but rather  $W_j^{(A)} T_A$ . Thus, for any given line, the absorber appears thinner than it really is. This must be kept in mind when determining the line broadening from the  $T_s = 0$  curves given in ref.<sup>5</sup>); that is, the apparent width can be written as  $\Gamma_a(0, W_j^{(A)} T_A)$ .

The recoilless fractions for this case can be determined by using the quantity

$$\varepsilon(\mathcal{S}_j) = \frac{P(\infty) - P(\mathcal{S}_j)}{P(\infty)} = f[1 - e^{-\frac{1}{2}W_j^{(A)} T_A} J_0(\frac{1}{2}i W_j^{(A)} T_A)] \quad (14)$$

in place of eq. (7).

### 2.3.3. Split emission and absorption spectra

When both emission and absorption lines are split by a hyperfine interaction, the transmission integral for a non-resonant absorbing source is given by eq. (8). Very little can be done with this general relation unless specific information, such as the number of source and absorber lines and their spacing and amplitudes, is known. Once such information is given, then the transmitted spectrum can be determined. In this section the results obtained for two specific cases are presented.

If the source and absorber line spacings are such that only one emission and absorption line interact at a time, then the resulting transmission spectrum will contain  $N_s \times N_A$  lines. If  $\mathcal{S}_{ij} = E_i^{(s)} - E_j^{(A)}$  is the Doppler shift required to produce exact coincidence of the  $j^{\text{th}}$  absorption line with the  $i^{\text{th}}$  emission line, then, in the vicinity of  $\mathcal{S}_{ij}$ ,

$$P(\mathcal{S} = \mathcal{S}_{ij} + \mathcal{S}'_{ij}) = [(1-f) + f \sum_{k \neq i} W_k^{(s)} + f W_i^{(s)} I(\mathcal{S}'_{ij}; W_j^{(A)} T_A)] P_{\text{non-res}}, \quad (15)$$

where  $|\mathcal{S}'_{ij}|$  is small as compared with

$$|E_i^{(s)} - E_{i+1}^{(s)}| \quad \text{and} \quad |E_j^{(A)} - E_{j+1}^{(A)}|.$$

Thus, each of the resonance lines produced by the overlap of a source line with an absorber line is approximately Lorentzian with width  $\Gamma_{ij} = \Gamma_a(0, W_j^{(A)} T_A)$  given by the curves for zero source thickness in ref.<sup>5)</sup>.

The recoilless fractions can be found from the relation

$$\varepsilon(\mathcal{S}_{ij}) = \frac{P(\infty) - P(\mathcal{S}_{ij})}{P(\infty)} = f W_i^{(s)} [1 - e^{-\frac{1}{2} W_j^{(A)} T_A} J_0(\frac{1}{2} i W_j^{(A)} T_A)]. \quad (16)$$

The effective recoilless fraction corresponding to the  $i^{\text{th}}$  emission line is thus  $f W_i^{(s)}$ , while the effective absorber thickness for the  $j^{\text{th}}$  absorption line is reduced to  $W_j^{(A)} T_A$ . This feature must be kept in mind when using the broadening curves of ref.<sup>5)</sup>.

The other specific case to be examined is the shape of the transmission curve appearing about zero Doppler shift for identical emission and absorption line spacings<sup>12)</sup>. Under these circumstances, at  $\mathcal{S} \simeq 0$  every emission line is absorbed strongly by a corresponding absorption line and eq. (8) reduces to

$$P(\mathcal{S} \simeq 0) = \left[ (1-f) + \sum_{i=1}^N f W_i^{(s)} I(\mathcal{S}; W_i^{(A)} T_A) \right] P_{\text{non-res}}. \quad (17)$$

Here, the resonance line is the sum of  $N$  lines, each approximately Lorentzian. Since the effective thickness for the  $i^{\text{th}}$  line is  $W_i^{(A)} T_A$ , the corresponding line width  $\Gamma_a(0, W_i^{(A)} T_A)$  can be found from the broadening curves of ref.<sup>5)</sup>. How closely the resulting resonance line approaches a Lorentz shape can be determined only by actually summing the individual lines. That is, the central resonance line can be approximated by the superposition

$$\sum_{i=1}^N \frac{W_i^{(s)}}{1 + [2\mathcal{S}/\Gamma_a(0, W_i^{(A)} T_A)]^2}, \quad (18)$$

and the width of this line can be empirically established.

This calculation has been performed for the 14.4 keV transition of Fe<sup>57</sup> split by a magnetic hyperfine interaction<sup>13-15)</sup>. Using component amplitudes corresponding to an unpolarized source and absorber, the resulting line was found to be approximately Lorentzian. The relative width of this line as a function of  $T_A$  is shown in fig. 1. The corresponding broadening for an unsplit line ( $\hbar(0, T_A)$  obtained from ref.<sup>5)</sup> is shown for comparison. Because of the reduction in effective thickness, the broadening is considerably smaller than for an unsplit transition.

The relation

$$\varepsilon(0) = \frac{P(\infty) - P(0)}{P(\infty)} = f \left[ 1 - \sum_{i=1}^N W_i^{(s)} e^{-\frac{1}{2} W_i^{(A)} T_A} J_0(\frac{1}{2} i W_i^{(A)} T_A) \right] \quad (19)$$

<sup>12)</sup> For the purpose of discussion it is assumed that the emission and absorption spectra overlap exactly at  $\mathcal{S} = 0$ . Since an isomeric shift may rigidly displace these spectra,  $\mathcal{S} = 0$  must be interpreted as the shift required to produce coincidence.

<sup>13)</sup> R. V. Pound and G. A. Rebka, Jr., Phys. Rev. Letters **3** (1959) 554.

<sup>14)</sup> G. DePasquali, H. Frauenfelder, S. Margulies and R. N. Peacock, Phys. Rev. Letters **4** (1960) 71.

<sup>15)</sup> S. S. Hanna, J. Heberle, C. Littlejohn, G. J. Perlow, R. S. Preston and D. H. Vincent, Phys. Rev. Letters **4** (1960) 177.

can be used to determine  $f$  and  $f'_A$ . It should be emphasized that eq. (19) and not (8) is applicable for the case of equally split emission and absorption spectra. Eq. (19), again evaluated for the split unpolarized 14.4 keV transition of  $\text{Fe}^{57}$ , is compared with eq. (8) in fig. 2. The consequences of reduced effective thickness are apparent.

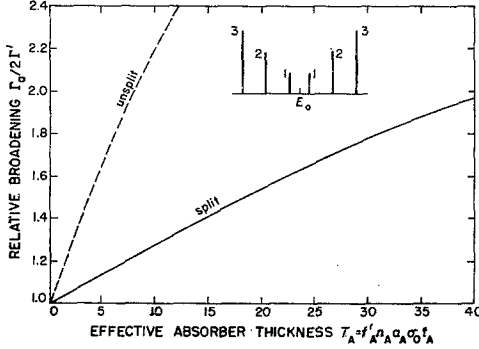


Fig. 1. Broadening of the central Mössbauer line for the split 14.4 keV transition in  $\text{Fe}^{57}$ . Component amplitudes corresponding to an unpolarized source and absorber are used. The broadening for the unsplit transition is shown for comparison.

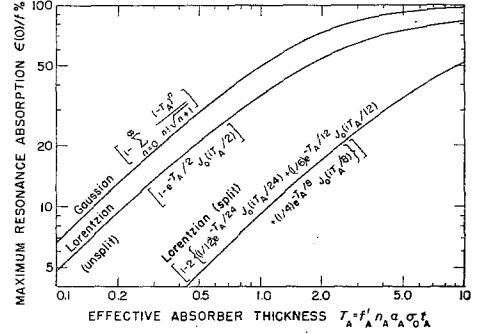


Fig. 2. Maximum resonance absorption as a function of absorber thickness. The quantity  $\epsilon(0)/\%$  is shown for Lorentzian (split and unsplit) and Gaussian (unsplit) spectral shapes. The split curve is calculated for the unpolarized source and absorber intensities shown in fig. 1.

#### 2.3.4. Non-Lorentzian spectra

In the previous sections, in discussing the transmission of resonance radiation, Lorentz shaped emission and absorption spectra have been assumed. While the calculations have not been restricted to lines of natural width, the broadened spectra have been taken to be Lorentzian. Although the mechanisms which broaden the emission and absorption lines are not yet well understood, it seems likely that in most cases the broadened lines will have non-Lorentzian shapes. To see the importance of spectral shape on the Mössbauer line, unsplit Gaussian emission and absorption spectra are investigated. Again, only non-resonantly absorbing sources are considered.

If the Gaussian emission and absorption lines are assumed to have the same width and to be centered about the energy  $E_0$ , then the shape of both lines is determined by the factor

$$\exp \left[ - \left( \frac{E - E_0}{\delta/2} \right)^2 \right].$$

Here,  $\delta$  represents the full width at  $1/e$  of the maximum intensity. In terms of  $\gamma$ , the width measured at half-maximum, this can be written as

$$\exp \left[ - \left( \frac{E - E_0}{\gamma/(2\sqrt{\ln 2})} \right)^2 \right].$$

For a broadened line  $\gamma$  is larger than  $\Gamma$ , the natural width of the transition. For such spectra the transmission, normalized according to eq. (2), is

$$P(\mathcal{S}) = \left\{ (1-f) + f \frac{2\sqrt{\ln 2}}{\gamma\sqrt{\pi}} \int_{-\infty}^{+\infty} dE \exp \left[ - \left( \frac{E - E_0}{\gamma/(2\sqrt{\ln 2})} \right)^2 \right] \exp \left[ - T_A e^{- \left( \frac{E - E_0 - \varphi}{\gamma/(2\sqrt{\ln 2})} \right)^2} \right] \right\} P_{\text{non-res}}. \quad (20)$$

The first and second terms of this equation represent, respectively, the transmission of the non-resonant and resonant fractions of the emitted radiation. In the resonant contribution the first part denotes the emission spectrum while the second part denotes the absorption in the external absorber. It should be noted that the factor  $\Gamma/T_A$  which appears in the expression for the cross section (see note<sup>6</sup>) must be replaced by  $\Gamma/\gamma$  to keep the total absorption constant.

The energy integral in eq. (20) can be evaluated by performing an expansion in powers of  $T_A$ . Thus,

$$P(\mathcal{S}) = \left\{ (1-f) + f \sum_{n=0}^{\infty} \frac{(-T_A)^n}{n! \sqrt{n+1}} \exp \left[ -\frac{n}{n+1} \left( \frac{\mathcal{S}}{\gamma/(2\sqrt{\ln 2})} \right)^2 \right] \right\} P_{\text{non-res}}. \quad (21)$$

For thin absorbers ( $T_A \ll 1$ ) this series can be evaluated in closed form by retaining only the first term in  $T_A$ :

$$P(\mathcal{S}) = \left\{ 1 - f \frac{T_A}{\sqrt{2}} \exp \left[ -\left( \frac{\mathcal{S}}{\sqrt{2} \gamma/(2\sqrt{\ln 2})} \right)^2 \right] \right\} P_{\text{non-res}}. \quad (22)$$

In this case the transmitted line shape is Gaussian but has an apparent width  $\gamma_a$  which is  $\sqrt{2}$  times larger than the width of either the emission or the absorption spectrum. This broadening, due to the preferential absorption of photons from the center of the emission line, is only  $\sqrt{2}$  times as great as in the corresponding Lorentzian case (cf. eqs. (5) and (9) of ref.<sup>3</sup>). Consequently, when starting with spectra of equal width the resulting Mössbauer line will be narrower for Gaussian lines than for Lorentzian lines.

Since the series appearing in eq. (21) could not be identified, an evaluation was performed on the University of Illinois digital computer ILLIAC. For values of  $T_A$  between zero and at least ten, the resulting transmitted line was found to approximate a Gaussian curve whose full width at half-height  $\gamma_a$  varies with the absorber thickness in accordance with the relation

$$\gamma_a = \sqrt{2} \gamma g(T_A). \quad (23)$$

The form of  $g(T_A)$ , the Gaussian broadening function, is shown in fig. 3. The corresponding Lorentzian broadening,  $h(0, T_A)$  obtained from ref.<sup>3</sup>, is also shown.

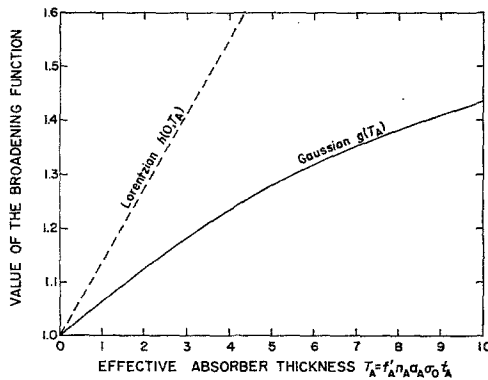


Fig. 3. Broadening of the transmitted line for Gaussian emission and absorption spectra. The broadening is calculated for a non-resonantly absorbing source. The corresponding Lorentzian broadening function is shown for comparison.

Upon comparing the line produced by the overlap of Gaussian spectra with that produced by Lorentzian spectra, it is seen that in either case the resulting line, while approximating the original spectral shape, is broadened. However, when starting with spectra of equal width, the resulting Gaussian line is not



only narrower but also broadens at a considerably slower rate than the corresponding Lorentzian line.

By procedures identical with those employed for Lorentzian spectra, the recoilless fraction for Gaussian spectra can be found by using the ratio

$$\varepsilon(0) = \frac{P(\infty) - P(0)}{P(\infty)} = f \left[ 1 - \sum_{n=0}^{\infty} \frac{(-T_A)^n}{n! \sqrt{n+1}} \right]. \quad (24)$$

The quantity  $\varepsilon(0)/f$ , representing the maximum resonance absorption in fractional form, is plotted in fig. 2. The Lorentzian (unsplit) and Gaussian absorption curves are essentially similar in shape but have one important difference: except in the asymptotic region where both curves approach unity, Gaussian spectra result in about 40% more resonance absorption than Lorentzian spectra.

From this brief discussion employing Gaussian spectra it can be concluded that the characteristics of the transmitted line are strongly dependent upon the shape of the emission and absorption spectra. Thus, when dealing with broadened Mössbauer lines, analyses based on a specific spectral shape must be applied with caution.

### 3. Experimental Arrangement

To test the predictions of the preceding section, measurements of the transmitted Mössbauer line as a function of absorber thickness were performed using the 14.4 keV radiation of  $\text{Fe}^{57}$ . The experiments were made with source and absorber combinations which were either unsplit or else identically split.

To obtain the required Doppler shift between the emission and absorption spectra, an inclined plane system (fig. 4) adapted from an Argonne National Laboratory design was used. In this device a reversible synchronous motor is employed to drive a carriage by means of an accurately machined lead-screw.

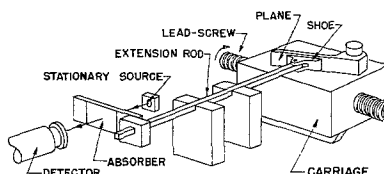


Fig. 4. Inclined plane device used to produce relative motion between source and absorber.

Mounted rigidly to the moving carriage is a plane whose angle of inclination can be continuously varied between  $0^\circ$  and  $45^\circ$ . A shoe pivoted to the foot of an extension rod slides smoothly along the inclined plane, being held quite firmly to the plane by a thin layer of oil. As the carriage is driven back and forth, the extension rod moves to-and-fro, carrying the absorber with it. In addition to the very fine speed control afforded by varying the incline angle, the lead-screw speed could be changed by a system of gears and pulleys not shown. With this arrangement the absorber velocity could be smoothly and accurately varied between 0 and  $1.52 \text{ cm/sec}^{16}$ .

A Philips X-ray counter was used to detect the 14.4 keV radiation. This detector was connected to the usual gamma-ray spectrometer consisting of a preamplifier, linear amplifier and single-channel pulse-height analyzer. A photoelectric device sensing the motion of the absorber was used to alternately switch the output of the analyzer into two scalars. The control circuit also switched pulses from a time-mark generator into two scalars, thereby determining the counting time for each channel. The control circuit in-

<sup>16)</sup> The device was calibrated by electronically measuring the time required to traverse a known distance for each of the gear-pulley combinations.

activated all scalars while the direction of motion was changing. In this manner the positive and negative velocity portions of the Mössbauer spectra were separated<sup>17)</sup>.

In addition to the 14.4 keV radiation, the gamma-ray spectrum of Fe<sup>57</sup> contains a line at 122 keV resulting from transitions from the second excited state. The amount of Compton-scattered 122 keV radiation falling into the 14.4 keV channel of the pulse-height analyzer was determined by interposing a  $\frac{1}{8}$ " aluminum sheet between the source and the counter and measuring the resulting "background" rate  $B$ . Specifically, the corrected counting rate at velocity  $v$  was found to be  $N_c(v) = N(v) - 1.083 B$ .

## 4. Experimental Results

### 4.1. UNSPLIT SPECTRA

To obtain an unsplit emission spectrum, a source was made consisting of Co<sup>57</sup> embedded in a 1 mil Type 310 stainless steel foil (composition: 55 % Fe, 25 % Cr, 20 % Ni<sup>18)</sup>). The activity was diffused at 1050° C for only 2 hours to insure a thin source. A series of Type 310 stainless steel absorbers of varying thicknesses were used in conjunction with this source. To investigate the effects of heating, a 1 mil absorber was given the same heat treatment as the source. No appreciable differences were found in the Mössbauer spectra measured before and after heating<sup>19)</sup>. Consequently, although the absorbers were untreated it is reasonable to assume that the internal environments in source and absorbers are essentially the same and that the emission and absorption lines are identical.

To determine the broadening due to resonance absorption in the external absorber, the transmitted line shape was measured for five absorbers of different thickness. In each case the line was measured at least five times. The results of a typical measurement obtained with a 22.2 mg/cm<sup>2</sup> absorber are shown in fig. 5.

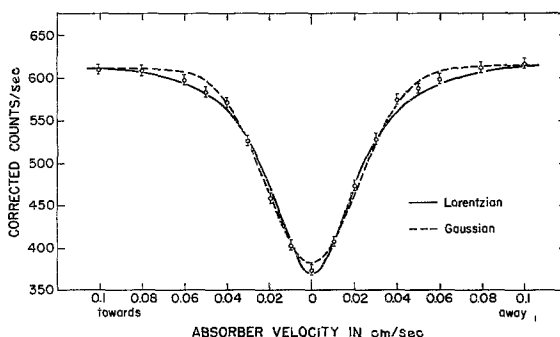


Fig. 5. Shape of the Mössbauer line obtained by using a source of Co<sup>57</sup> embedded in Type 310 stainless steel with a 22.2 mg/cm<sup>2</sup> Type 310 absorber. The Lorentzian and Gaussian curves shown have been fitted to the experimental points by a least-squares analysis.

Also shown are a Lorentzian and a Gaussian curve, each fitted to the experimental points by a least-squares analysis. Neither curve provides an exact fit. The deviation from a Lorentz shape is not surprising since the line is considerably broader than the natural width<sup>20)</sup>. ( $\Gamma = 9.5 \times 10^{-2}$  cm/sec).

Because the shape of the observed line is neither Lorentzian nor Gaussian, an unambiguous comparison of theory with experiment is impossible. Nevertheless it is valuable to apply the results obtained for the

<sup>17)</sup> The transmission at  $+v$  and  $-v$  can not, in general, be added because an isomeric shift, displacing the emission and absorption spectra, is often present.

<sup>18)</sup> G. K. Wertheim, Phys. Rev. Letters **4** (1960) 403.

<sup>19)</sup> This is in sharp contrast to results obtained with iron sources and absorbers. Apparently, the line in Type 310 stainless steel is already broadened so much by some other mechanism that the effects of annealing are negligible (see ref. <sup>18)</sup> and <sup>20)</sup>).

<sup>20)</sup> G. K. Wertheim, Phys. Rev. **123** (1961) 755.

Lorentzian and Gaussian cases to the experimental data in order to see the variations in the quantities involved. Only the analysis based on the definitions of  $\epsilon(0)$  and  $T_A$  will be presented<sup>21</sup>).

To estimate the fraction of atoms which emit and absorb gamma rays without recoil, the experimental values of the maximum resonance absorption

$$\epsilon_{\text{exp}}(0) = \frac{N_c(\infty) - N_c(0)}{N_c(\infty)} \bigg|_{\xi_A} \quad (25)$$

were plotted as a function of the absorber thickness  $\xi_A$  (expressed in  $\text{mg}/\text{cm}^2$ ) on log-log paper. Curves of  $\epsilon(0)/f$  vs.  $T_A$ , as given by eqs. (7) and (24), were also plotted on log-log paper. Since  $\epsilon_{\text{exp}}(0)$  and  $\xi_A$  are proportional, respectively, to  $\epsilon(0)/f$  and  $T_A$ , the experimental and calculated curves can be brought into

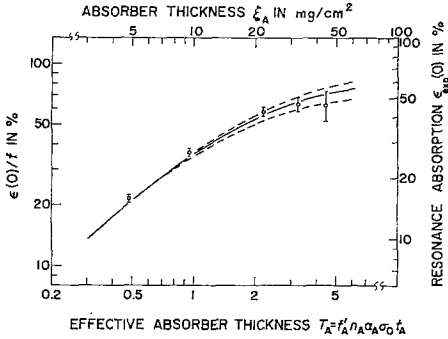


Fig. 6. Resonance absorption for a single-line source and absorber. The source consists of  $\text{Co}^{57}$  diffused into Type 310 stainless steel. The absorbers are also Type 310 steel. The experimental data are fitted to the curve calculated on the assumption of Lorentzian spectra. Although the extreme limits of the fit are indicated by the broken lines, the coordinate calibration is valid only for the solid line.

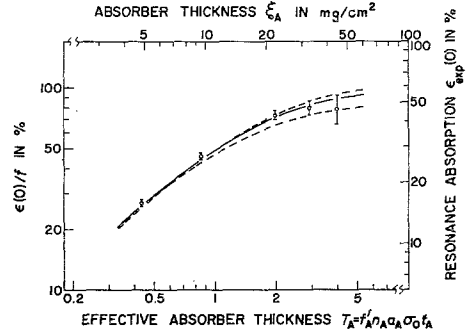


Fig. 7. Resonance absorption for a single-line source and absorber. The source consists of  $\text{Co}^{57}$  diffused into Type 310 stainless steel. The absorbers are also Type 310 steel. The experimental data are fitted to the curve calculated on the assumption of Gaussian spectra. Although the extreme limits of the fit are indicated by the broken curves, the coordinate calibration is valid only for the solid curve.

coincidence by a coordinate translation. (figs. 6 and 7). Once such a fit has been made,  $f$ , the fraction of recoilless emissions, as well as  $T_A/\xi_A$ , the ratio of effective to actual absorber thickness, follow immediately. Now,  $t_A$  (the thickness in cm) and  $\xi_A$  (the thickness in  $\text{mg}/\text{cm}^2$ ) are connected by

$$\xi_A = n_A A t_A, \quad (26)$$

where  $n_A$  is the number of atoms/ $\text{cm}^3$  and  $A$  is the average atomic mass of the absorber material. The effective thickness can then be expressed as

$$T_A = f'_A n_A a_A \sigma_0 t_A = f'_A a_A \sigma_0 \xi_A / A. \quad (27)$$

A knowledge of the ratio  $T_A/\xi_A$  thus serves to determine  $f'_A$ , the fraction of recoilless absorptions, provided that the factors  $\Gamma/\Gamma_A$  (for the Lorentzian case) and  $\Gamma/\gamma_A$  (for the Gaussian case) which appear

<sup>21</sup>) The more precise procedure of Shirley *et al.*<sup>9)</sup> which makes use of the line broadening relations of eq. (4) or (23) in addition to the definitions of  $\epsilon(0)$  and  $T_A$ , gives inconsistent results in this case. This follows from the fact that the actual broadening is not as predicted by these equations.

in the expression for  $\sigma_0$  are known. Making use of the line broadening data (to be discussed later), the following results are obtained:

Spectral shape	$T_A/\xi_A$	$f(\%)$	$f'_A(\%)$
Lorentzian	$0.10 \pm \begin{smallmatrix} 0.02 \\ 0.01 \end{smallmatrix}$	$74 \pm \begin{smallmatrix} 10 \\ 7 \end{smallmatrix}$	$121 \pm \begin{smallmatrix} 15 \\ 8 \end{smallmatrix}$
Gaussian	$0.09 \pm \begin{smallmatrix} 0.02 \\ 0.01 \end{smallmatrix}$	$59 \pm \begin{smallmatrix} 9 \\ 5 \end{smallmatrix}$	$153 \pm \begin{smallmatrix} 15 \\ 8 \end{smallmatrix}$

The rather large uncertainties associated with each of the above quantities result from the fact that the curves of eqs. (7) and (24) vary only slowly with  $T_A$ . Thus, a considerable degree of latitude exists in fitting the experimental points to the predicted curves. (See figs. 6 and 7.)

A surprising feature of the results is that  $f'_A$  is greater than 100% on the basis of both Lorentzian and Gaussian spectral shapes. The most plausible explanation for this anomalous result is that the value of the conversion coefficient given in the literature<sup>22)</sup> is too large. The fact that Lynch *et al.*<sup>23)</sup> and Wu *et al.*<sup>24)</sup> have found that the effective absorber thickness, calculated on the basis of  $\alpha = 15$ , seems to be smaller than the actual value, lends credence to this hypothesis. The reasonable assumption that  $f'_A \sim 70\%$  indicates that the conversion coefficient should have a value of approximately 8.

The correct values of the Mössbauer parameters for Type 310 stainless steel probably lie somewhere between the values found by applying the calculation for Lorentzian and Gaussian spectra to the experimental data. Simply averaging these results yields  $T_A/\xi_A = 0.095$ ,  $f = 67\%$ . Although the value of  $f'_A$  depends upon  $\alpha$ , it seems likely that  $f'_A$  and  $f$  are equal since the source and absorbers are essentially identical.

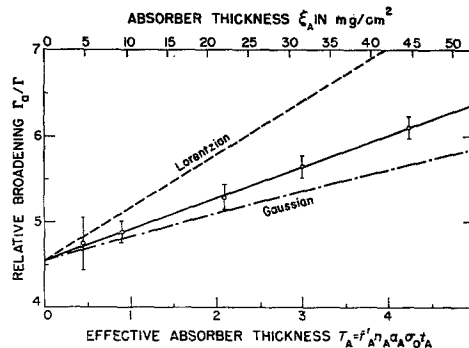


Fig. 8. Relative broadening for a single-line source and absorber. The source consists of  $\text{Co}^{57}$  diffused into Type 310 stainless steel. The absorbers are also Type 310 steel. The broadening expected for Lorentzian and Gaussian spectra is shown. These calculated curves are adjusted to fit the experimental data at  $T_A = 0$ .

To investigate the line broadening due to resonance absorption in the external absorber it is necessary to plot the ratio of experimentally determined line width to natural width as a function of  $T_A$ , and to compare these points with the curves predicted by the calculations. Such a comparison, made using the average value  $T_A/\xi_A = 0.095$ , is shown in fig. 8<sup>25)</sup>. The theoretical curves [ $\Gamma_a/\Gamma = (2\Gamma'/\Gamma)h(0, T_A)$  for

<sup>22)</sup> H. R. Lemmer, O. J. A. Segaert and M. A. Grace, Proc. Phys. Soc. (London) **68** A (1955) 701.

<sup>23)</sup> F. J. Lynch, R. E. Holland and M. Hamermesh, Phys. Rev. **120** (1960) 513.

<sup>24)</sup> C. S. Wu, Y. K. Lee, N. Benczer-Köller and P. Simms, Phys. Rev. Letters **5** (1960) 432.

<sup>25)</sup> The measured values of the width have been corrected for the small velocity spread resulting from the finite solid angle subtended by the detector.

the Lorentzian case and  $\gamma_a/\Gamma = (\sqrt{2} \gamma/\Gamma)g(T_A)$  for the Gaussian case] have been adjusted to coincide with the least-squares line through the experimental points at  $T_A = 0$ . As expected, the experimental points fall between the two theoretical curves. Since both  $h(0, T_A)$  and  $g(T_A)$  approach unity as  $T_A$  approaches zero, the value of the relative broadening at zero absorber thickness can be used to estimate the width of the presumably identical emission and absorption spectra:  $\Gamma'/\Gamma = 2.28$  (Lorentzian);  $\gamma/\Gamma = 3.23$  (Gaussian). The actual width probably lies between these values.

#### 4.2. IDENTICALLY SPLIT SPECTRA

To test the results developed for identically split emission and absorption spectra, a source consisting of  $\text{Co}^{57}$  co-plated with stable  $\text{Fe}^{56}$  onto a 0.001 in. Armco iron backing was used in conjunction with a series of Armco absorbers. This source, although non-resonantly absorbing, is ferromagnetic as are the absorbers. As a consequence of the resulting hyperfine interaction, the 14.4 keV transition is split into six components<sup>15</sup>). Both the source and the absorbers were carefully annealed so that the assumption of identical emission and absorption spectra is not unreasonable<sup>26</sup>).

In these experiments, the shape of the central resonance line was measured at least five times with each absorber. Unlike the stainless steel results, the observed line shapes, although somewhat broadened, were approximately Lorentzian. Consequently, the experimental data need be compared only with the results obtained for Lorentzian spectra. The width and depth of every resonance line was determined by fitting a least-squares Lorentz curve to the experimental points, and the individual values for each absorber were averaged.

In accordance with the method described previously, the recoilless fractions  $f$  and  $f'_A$  can be obtained by fitting the experimental points corresponding to the amount of resonance absorption exhibited by the central line to the curve given by eq. (19). In evaluating this equation, the component intensities for an

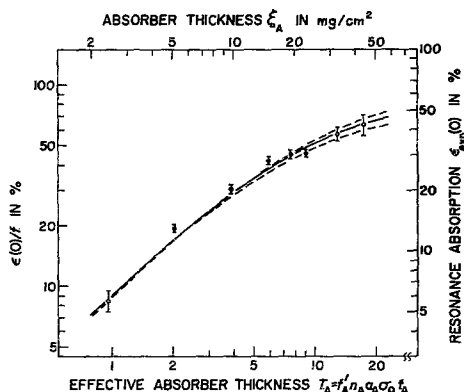


Fig. 9. Resonance absorption of the central Mössbauer line produced by an identically split source and absorber. The source consists of  $\text{Co}^{57}$  embedded in stable  $\text{Fe}^{56}$ , while the absorbers are of Armco iron. The experimental data are fitted to curves based on the assumption of Lorentz shaped emission and absorption components. Component intensities corresponding to an unpolarized source and absorber have been used. Although the extreme limits of the fit are indicated by the broken curves, the coordinate calibration is valid only for the solid curve.

unpolarized source and absorber were used. The fit shown in fig. 9 results in the following values:  $T_A/\xi_A = 0.40 \pm 0.05$ ;  $f = (67 \pm 7)\%$ . By employing the line broadening data yet to be discussed,  $f'_A$  is found to be  $(144 \pm 15)\%$ . This spurious value, consistent with that obtained with Type 310 stainless steel, tends

<sup>26</sup>) This assumption is supported by the fact that the emission and absorption spectra seem to be only about 25% wider than the natural width.

to confirm the existence of an error in at least one of the physical constants appearing in the expression for  $T_A$ . The hypothesis that the conversion coefficient is approximately 8 rather than 15 reduces  $f'_A$  to a more reasonable value.

When the emission and absorption spectra are split identically, the width of the resulting central resonance line can no longer be found directly from the broadening curves given in ref.<sup>5</sup>). In such cases the central line consists of the sum of a series of lines, each produced by the overlap of an emission component with the same absorption component. Such a superposition (eq. 18) has been performed for the split 14.4 keV transition, and the resulting line broadening is shown in fig. 1. A knowledge of the ratio  $T_A/\xi_A$  allows the experimentally observed broadening to be compared with the predicted values. Using  $T_A/\xi_A = 0.40$  yields the results shown in fig. 10. The curve drawn through the points is the least-squares straight line. The theoretical curve has been normalized so as to intersect this line at  $T_A = 0$ . Assuming identical emission and absorption spectra, the extrapolation to zero thickness yields  $\Gamma'/\Gamma = 1.24$  as the relative width of both spectra.

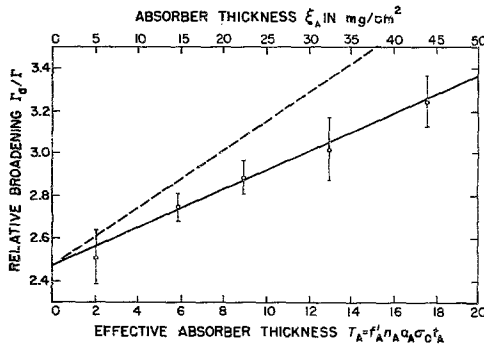


Fig. 10. Broadening of the central line for identically split source and absorber. The source consists of  $\text{Co}^{57}$  embedded in stable  $\text{Fe}^{56}$ . The absorbers are Armco iron. The broadening expected for Lorentzian spectra, adjusted to fit the experimental data at  $T_A = 0$ , is also shown.

As seen in fig. 10, the experimental points lie somewhat below the calculated curve. This behavior is not surprising in view of the strong dependence of the broadening function on the shape of the spectral lines. The fact that the lines seem to be broadened to almost 125% of their natural width indicates a departure from the pure Lorentz shape assumed in the calculations. In addition, the summation of individual Lorentzian components to form the composite line is only an approximation.

## 5. Summary

Since the great utility of the Mössbauer effect arises from the fact that very narrow resonance lines can be observed, a consideration of the transmitted line shape is of interest. The shape of the Mössbauer lines to be expected in a transmission-type experiment has been discussed in a recent paper<sup>5</sup>). There, an integral expressing the transmission of resonance radiation emitted from a source of finite thickness and passing through an external resonance absorber is examined. Empirically, it was found that for Lorentzian emission and absorption spectra the transmitted line is approximately a Lorentz curve whose width increases with increasing source and absorber thickness. This line broadening is presented graphically for both uniform and Gaussian source distributions.

To increase their usefulness, these calculations have been extended in the present work to the case where the emission and absorption lines are split by a hyperfine interaction. In addition, to see the effects of spectral shape, Gaussian emission and absorption lines have been considered. The results indicate that

the characteristics of the transmitted line are strongly dependent upon the spectral shape. Thus, when dealing with broadened (and therefore probably distorted) Mössbauer lines, analyses based on simple spectral shapes must be applied with discrimination.

To test the calculations, a series of experiments were performed in which the transmitted line shape was measured as a function of absorber thickness. These experiments were performed using the  $\text{Fe}^{57}$  14.4 keV radiation. To obtain unsplit emission and absorption spectra, Type 310 stainless steel was used for both source backing and absorbers. The observed line was more than four times as wide as the natural width and was neither Lorentzian nor Gaussian in shape. Consequently, an unambiguous comparison of theory with experiment is impossible. Averaging the results obtained from the Lorentzian and Gaussian analyses yields  $f = 67\%$ ,  $f'_A = 137\%$  for the source and absorber recoilless fractions. The anomalously large value of  $f'_A$  seems to indicate that the conversion coefficient for the 14.4 keV transition is not 15, but rather, about 8. Identically split spectra were obtained by using Armco iron for both source backing and absorbers. In this case the central resonance line was approximately Lorentzian in shape. Applying the Lorentzian analysis results in the values  $f = (67 \pm 7)\%$ ,  $f'_A = (144 \pm 15)\%$ . Again,  $f'_A$  can be reduced to a reasonable value by assuming a conversion coefficient of approximately 8.

### Acknowledgements

We are indebted to G. K. Wertheim for supplying the Type 310 stainless steel foils, to G. De Pasquali for performing the source preparations and absorber heat treatments, and to R. J. Namtvedt for designing much of the mechanical equipment. We would also like to thank P. Axel, J. R. Ehrman, J. H. Hetherington and D. G. Ravenhall for many constructive discussions. One of us (S.M.) wishes to thank the U.S. Air Force Office of Scientific Research and the National Academy of Sciences-National Research Council for support during the writing of this paper.